

Fig. 2 Triangular region used in computation.

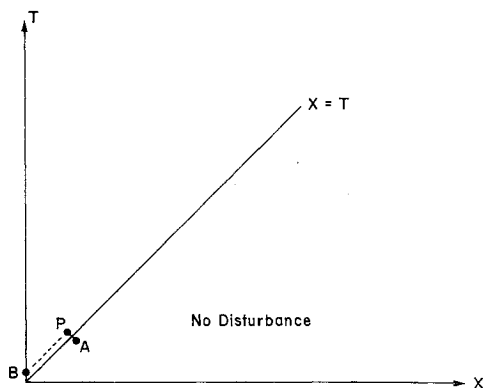
$\pm 1$  along the lines  $dT/dX = \pm 1$ , whereas the modified shear wave is propagated with dimensionless velocities  $\pm \delta$  along the lines  $dT/dX = \pm 1/\delta$ . Since the dilatational wave velocity is larger than that of the modified shear wave and the rod is quiescent initially, there is no disturbance before the dilatational wave, excited by the step pressure at the end  $x = 0$ , arrives.

A finite-difference procedure for the numerical integration of Eqs. (7-9) has been performed on the grid formed by the characteristics of the dilatational wave family. A typical element† of the grid is shown in Fig. 1. If  $U_x$ ,  $U_T$ ,  $W_x$ ,  $W_T$ , and  $U$  are given at  $D$ ,  $A$ , and  $B$ , those values at  $P$  can be found from Eqs. (7-9) by the numerical procedure. By successive use of this procedure, all values at grid points  $A_{01}$ ,  $A_{02}$ , ...,  $A_{0n}$ ;  $A_{11}$ ,  $A_{12}$ , ...,  $A_{1n}$ ; ...;  $A_{nn}$  in Fig. 2 can be evaluated.

The only discontinuity of the boundary and initial conditions is at the origin ( $X = T = 0$ ), since the input axial pressure at  $X = 0$  is a step function. This discontinuity is propagated along the characteristic  $X = T$  and makes  $W_x$  and  $W_T$  among the five dependent variables  $W_x$ ,  $W_T$ ,  $U_x$ ,  $U_T$ , and  $U$  discontinuous across it. From Eq. (10), since  $U$  is continuous, the dimensionless magnitude of the jump for  $W_x$  at the origin is

$$P_D = 2P_0/a^2(\lambda + 2\mu) \quad (11)$$

By establishing Eqs. (7a, b) along  $BP$  and  $AP$ , respectively, where  $B$ ,  $P$ , and  $A$  are arbitrarily close to the line  $X = T$  as shown in Fig. 3, one knows that  $W_x$ , as well as  $-W_T$ , has a discontinuity of magnitude  $P_D$  across the characteristic  $X = T$  at the origin, and it is propagated along  $X = T$  without change of magnitude.

Fig. 3 Line of discontinuity  $X = T$ .

† At the boundary, the element becomes a triangle  $PBD$ . If those values at  $B$ ,  $D$ , and two of the five values at  $P$  are given, the three others at  $P$  can be determined by Eqs. (7b, 8b, and 9).

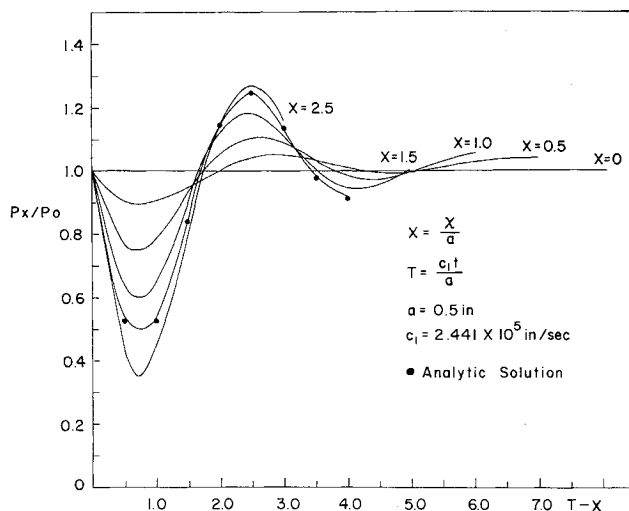


Fig. 4 Axial-rod stress with time at various stations.

### Numerical Example

A numerical example based upon this method is given below for the following data:

$$\nu = 0.325 \quad \kappa_1 = 0.767 \quad \kappa^2 = 0.8667$$

$$a = 0.5 \text{ in.} \quad \Delta T = 0.01$$

where  $\Delta T$  is the dimensionless time interval to be taken in the numerical integration. The result is shown in Fig. 4. At each station  $X = 0.5, 1.0, 1.5, 2.0$ , and  $2.5$ , the axial-rod stress ratio  $P_x/P_0$  is plotted vs time duration  $(T - X)$  after the dilatational wave has arrived. An analytic solution from Ref. 2 is also plotted in the same figure as a check of the direct numerical solution.

### Discussion

The numerical technique used in this problem is quite simple. The grid is formed by characteristics that have the smallest magnitude in slope. For this reason, the numerical method is automatically stable. In the process of computation,  $W_x$ ,  $W_T$ ,  $U_x$ ,  $U_T$ , and  $U$ , i.e., stresses and displacements, can be found at the same time; the analytic methods do not have this advantage.

This method can be extended to all transient vibration problems of the continued system as long as the governing equation of motion is hyperbolic. One of the most important examples is that of a semi-infinite cylindrical shell with consideration of the rotatory inertia and shear deformation.<sup>7</sup> The nonhomogeneous equation can be treated without difficulty by means of this method.

The only disadvantage of this method is the long computer time required, even on a large-scale digital computer, such as the IBM 7090. In this example, the dispersion is very obvious within a short time, so that computing time is not long. For the same problem on a thin-walled shell, a longer time must be allowed if the apparent dispersion is to be obtained.

### References

- Mindlin, R. D. and Herrmann, G., "A one-dimensional theory of compressional waves in an elastic rod," *Proceedings of the First U. S. National Congress of Applied Mechanics, June, 1951* (American Society of Mechanical Engineers, New York, 1952), pp. 187-191.
- Miklowitz, J., "The propagation of compressional waves in a dispersive elastic rod, Part I—Result from the theory," *J. Appl. Mech.* **24**, 231-239 (1957).
- Kaul, R. K., "On the propagation of pressure pulses in circular elastic rods," *Z. Angew. Math. Phys.* **14**, 704-712 (1963).

<sup>4</sup> Petrovsky, I. G., *Lectures on Partial Differential Equations*, transl. by A. Shenitzer (Interscience Publishers, Inc., New York, 1954), 1st English ed., Chap. I.

<sup>5</sup> Leonard, R. W. and Budiansky, B., "On traveling waves in beams," NACA TN 2874 (1953).

<sup>6</sup> Plass, H. J., Jr., "Some solutions of the Timoshenko beam equation for short pulse-type loading," J. Appl. Mech. 25, 379-385 (1958).

<sup>7</sup> Tang, S. C., "Dynamic response of a thin-walled cylindrical tube under internal moving pressure," Ph. D. Thesis, Univ. of Michigan (1963).

## Altitude-Velocity Charts for Imperfect Air

CLARK H. LEWIS\* AND E. G. BURGESS III†  
 ARO, Inc., Arnold Air Force Station, Tenn.

NUMEROUS authors have computed normal shock-wave parameters based on perfect gas† thermodynamic properties and various "standard" atmospheres (e.g., see Feldman,<sup>1</sup> Wittliff and Curtis,<sup>2</sup> and Marrone<sup>3</sup>). At sufficiently low pressures, except for changes in standard atmosphere conditions, those results should be sufficiently accurate for most engineering purposes. However, at high pressures (or more correctly at high densities), the effects of intermolecular forces can become important and the thermodynamic properties are affected.

Lewis and Burgess<sup>4</sup> recently computed freestream stagnation conditions, conditions behind a normal shock, and nor-

Table 1 Ranges of conditions considered in altitude-velocity calculations

Altitude-velocity ranges			
	Model atmosphere	Altitude range, kft	Velocity range, kft/sec
Wittliff and Curtis	1959	0-300	2-26
Marrone	1959	0-300	26-50
Lewis and Burgess	1962	10-400	6-50

### Gasdynamic properties<sup>a</sup>

Wittliff and Curtis<sup>b</sup> and Marrone<sup>b</sup>:  $\rho_s/\rho_1$ ,  $p_s/p_1$ ,  $T_s/T_1$ ,  $Z_s/H_1$ ,  $H_0'/H_1$ ,  $p_0'/p_1$ ,  $T_0'/T_1$ ,  $\gamma_e^c$

Lewis and Burgess:

$$\begin{aligned} & H_0/H_1, p_0/p_1, \rho_0/\rho_1, T_0/T_1, a_0/a_1, Z_0, \gamma_{E,0s}^d \\ & H_s/H_1, p_s/p_1, \rho_s/\rho_1, T_s/T_1, S_s/R, Re_1/\text{ft}, \gamma_{E,s} \\ & q(\tau_n)^{1/2}, p_0'/p_1, \rho_0'/\rho_1, T_0'/T_1, a_0'/a_1, Z_0', \gamma_{E,0'} \end{aligned}$$

<sup>a</sup> Subscript 1 denotes freestream, s behind normal shock, 0 freestream stagnation, 0' normal shock stagnation, and a at 273.15°K and 1 atm.

<sup>b</sup> Gas composition behind the normal shock also given based on 14 specie model.

<sup>c</sup>  $\gamma_e = 2M_1^{-2} (\rho_1/\rho_s - 1)^{-1} - 1$ .

<sup>d</sup>  $\gamma_E = (\partial \ln p / \partial \ln p)_s$ .

Received December 10, 1964. This work was sponsored by the Arnold Engineering Development Center (AEDC), Air Force Systems Command, U. S. Air Force, under Contract No. AF 40(600)-1000 with ARO, Inc., Operating Contractor, AEDC.

\* Engineer, Hypervelocity Branch, von Karman Gas Dynamics Facility. Member AIAA.

† Member, Scientific Computing Branch, Engineering Support Facility.

‡ The ideal gas obeys  $p = \rho RT$ ,  $h = C_p T$ , and  $\gamma = C_p/C_v = \text{const}$ . A perfect gas will denote one obeying  $p = Z\rho RT$ , which includes dissociation and ionization neglecting intermolecular effects. An imperfect gas obeys  $p = Z\rho RT$ , which includes dissociation, ionization, and intermolecular forces. Local thermodynamic [i.e., thermal, mechanical (pressure), and chemical] equilibrium is assumed to exist for all conditions.

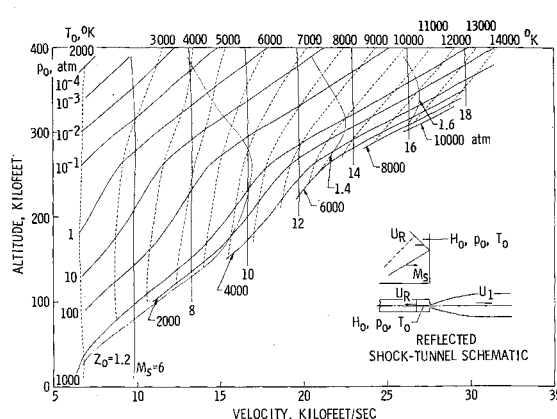


Fig. 1 Equilibrium freestream stagnation conditions necessary for flight duplication.

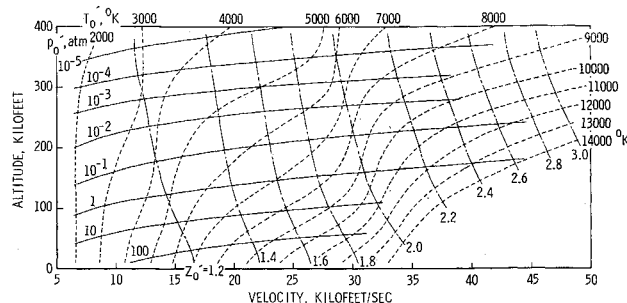


Fig. 2 Normal shock stagnation conditions at flight duplication.

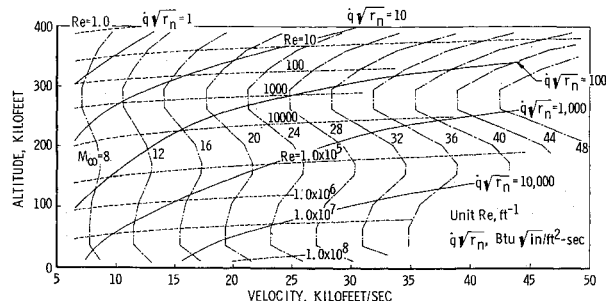


Fig. 3 Freestream Mach number, unit Reynolds number, and Fay-Riddell stagnation heat-transfer rate at flight duplication.

Table 2 Comparison of Air Research and Development Command (1959) and U. S. Standard (1962) model atmospheres<sup>a</sup>

Geo-metric alt., kft	$p_1$	$\rho_1$	$T_1$	$H_1/R^b$	$a_1^b$
0	...	...	...	-0.4	...
70	-0.06	0.52	-0.57	-1.06	-0.32
100	-0.8	-3.16	2.50	2.00	1.21
120	2.44	-1.58	4.12	3.62	2.00
160	9.41	4.77	4.45	5.98	2.15
170	11.2	6.45	4.34	3.98	2.15
200	14.1	16.09	-1.75	-2.22	-0.92
220	11.15	15.5	-3.76	-4.21	-1.93
250	2.74	10.2	-6.74	-7.16	-3.45
280	-11.25	-2.96	-8.29	-8.70	-4.27

<sup>a</sup> Data shown were computed from percent difference =  $100 [x(1959) - x(1962)]/x(1962)$ .

<sup>b</sup>  $H(1959)$  and  $a(1959)$  were obtained from Wittliff and Curtis.<sup>2</sup>